ELSEVIER

Nuclear Instruments and Methods in Physics Research A 430 (1999) 277–291

NUCLEAR INSTRUMENTS & METHODS IN PHYSICS RESEARCH Section A

www.elsevier.nl/locate/nima

Electron drift velocity measurements in liquid krypton–methane mixtures

M. Folegani[a,b], P.L. Frabetti[c], M. Magri[a,b], L. Piemontese[a,*]

[a] *Istituto Nazionale di Fisica Nucleare, Sezione di Ferrara, 44100 Ferrara, Italy*
[b] *Dipartimento di Fisica, Università di Ferrara, 44100 Ferrara, Italy*
[c] *Istituto Nazionale di Fisica Nucleare, Sezione di Bologna and Dipartimento di Fisica, Università di Bologna, Bologna, Italy*

Received 3 November 1998; received in revised form 26 January 1999

Abstract

Electron drift velocities have been measured in liquid krypton, pure and mixed with methane at different concentrations (1–10% in volume) versus electric field strength, and a possible effect of methane on electron lifetime has been investigated. While no effect on lifetime could be detected, since lifetimes were in all cases longer than what measurable, a very large increase in drift velocity (up to a factor 6) has been measured.

1. Introduction

Liquefied noble gases (called noble liquids in the following), in which ionization is measured, have been studied as particle detectors since the 1960s [1], and are now an important tool as active elements in precision electromagnetic calorimetry in various current high-energy experiments [2–4]. Furthermore, the use of noble liquids in time projection chambers (TPC) has been proposed for the detection and measurement of such processes as proton decay, double beta decay, and solar neutrino flux [5].

Such success has happened in spite of some obvious disadvantages such as the need for cryogenics, vessels and especially the slow response: the measurement of ionization in a liquid is a process which can take a few μs. Modest is therefore the time resolution that can be achieved with such detectors. The time necessary to collect all the free electrons in the active volume and to process the signal through the electronics chain are bound by the primary physical process: the drift of electrons through the liquid and its velocity. Such velocity can be a serious limit in some experiment, especially given the trend towards high-intensity accelerators and colliders: in fact both the probability of pile-up and the time resolution can be too large.

Various ways to alleviate, reduce or solve the problem have been proposed, based on the reduction of the size of the basic calorimeter cell, to reduce in each the average occupancy; or based on shorter and shorter signal shaping times. Another approach, which is pursued in this work, consists in

* Corresponding author. Tel.: + 39-532-78-1867; fax: + 39-532-76-20-57.
E-mail address: livio@fe.infn.it (L. Piemontese)

0168-9002/99/$ - see front matter
PII: S0168-9002(99)00181-3

mixing with the noble liquid (krypton in this case) small percentages of some additive (methane in our case) which can increase significantly the electron velocity.

It has been already shown [6–9] that in liquid argon and xenon the addition of solute hydrocarbons increases the drift velocity far above the saturation value. The effect can be roughly explained – for large values of the electric field – by a decrease of the average temperature of the drifting electrons, which entails a longer mean free time between successive collisions with the liquid atoms (molecules).

While at high fields the increase of the drift velocity can be very useful for applications in calorimetry, precise measurements also at low electric fields can be useful for the understanding of transport phenomena in liquids [10].

In this paper we will present results for fields from 10 to 9000 V/cm.

2. Detector design

2.1. Ionization chamber

We have used for these measurements a ionization chamber in which the drifting electrons are photoextracted from the cathode by a flash of UV light. The electrons drift through the electrostatic structure of the chamber until they are collected by the anode. The chamber has three substructures separated by two grids, as shown in Fig. 1. The three regions have of course three different values of electric field to ensure full transparency of the grids to the drifting electrons [11]. This structure serves two purposes. In the first place, to measure the electron lifetime we have to compare the charge emitted by the cathode with that collected by the anode: two independent charge measurements on the two electrodes may be obtained only if they are electrostatically screened.

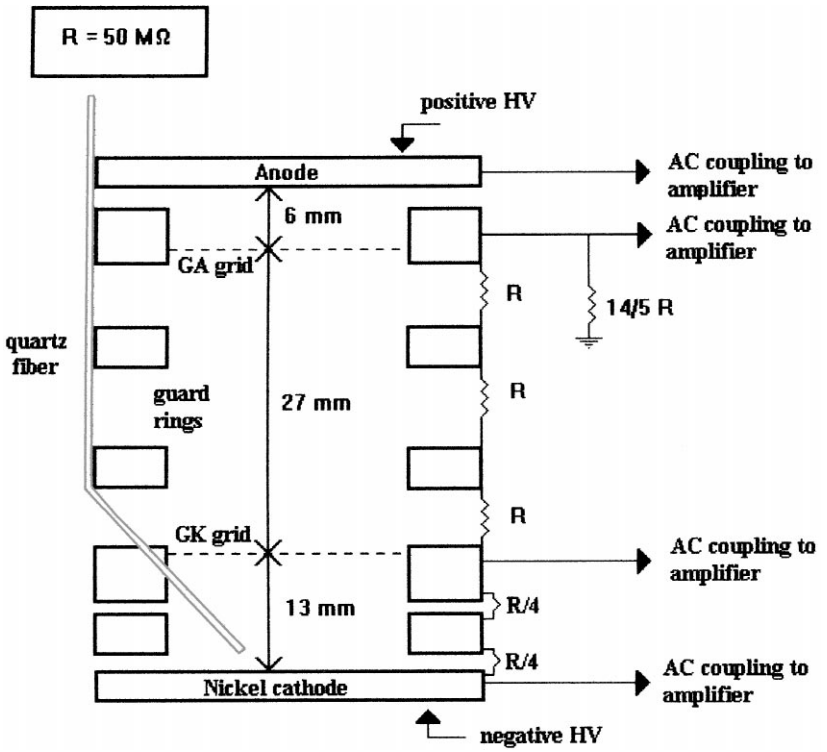

Fig. 1. Electric structure of the ionization chamber.

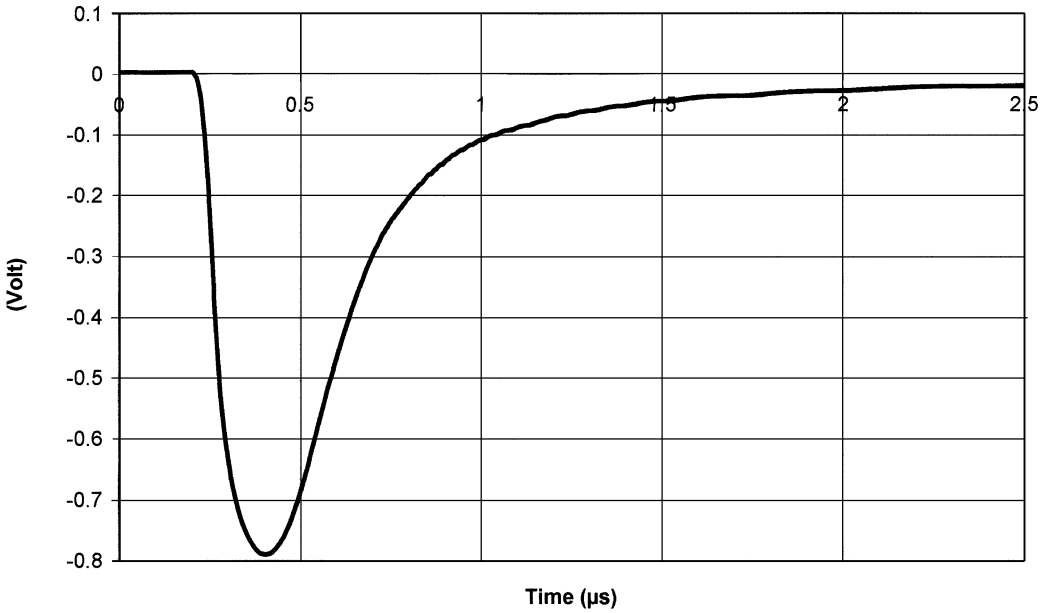

Fig. 2. Photomultiplier pulse from the light of one xenon lamp shot.

Moreover, with long and short drift regions we can measure drift velocity in different ranges of electric field with a reasonable value of the applied high voltage.

The basic electrostatic structure (cathode, two grids and anode) is completed by three guard rings whose purpose is to keep the electric fields uniform inside the drift regions.

UV light, brought into the chamber by a quartz optical fibre, is generated by a xenon lamp. The wavelengths of the emitted spectrum vary from 160 to 2000 nm, with two peaks at 230 and 250 nm. Using a lamp instead of a laser (for cost reasons) entails having a wide light pulse (360 ns FWHM): its shape, as collected by a photomultiplier located near the lamp, is presented in Fig. 2. The cathode, from which the UV flash extracts the electrons, is coated with nickel since tests have demonstrated its superior efficiency over other standard metals.

Two thermoresistances, located one below the cathode and the other above the anode, provide constant monitoring of temperature.

2.2. Gas system purification and cryogenics

In Fig. 3 a schematic drawing of the gas purification system and cryogenics is shown. The detection and measurement of a possible effect of methane on electron lifetime requires that we have a low level of electronegative pollutants released in the krypton gas or liquid by surface outgassing or other sources. The gas mixtures are provided by industry [12], and the relative precision in methane concentration is about 2%. The gas is liquefied in the measurement cell, after passing through a chemical trap (oxysorb, [12]) which absorbs traces of water and oxygen. The cooling and its thermal regulation are provided by immersion of the measurement cell into a bath of isopentane cooled with liquid nitrogen, which provides a large thermal inertia.

The piping is entirely made of stainless steel; in the construction of the ionization chamber steel, ceramics, Kapton, Teflon and HV resistors on ceramic substrate have been employed, due to their good bakeability and low outgassing. The chamber has been baked under vacuum at $\sim 100^{\circ}$C for at least a day.

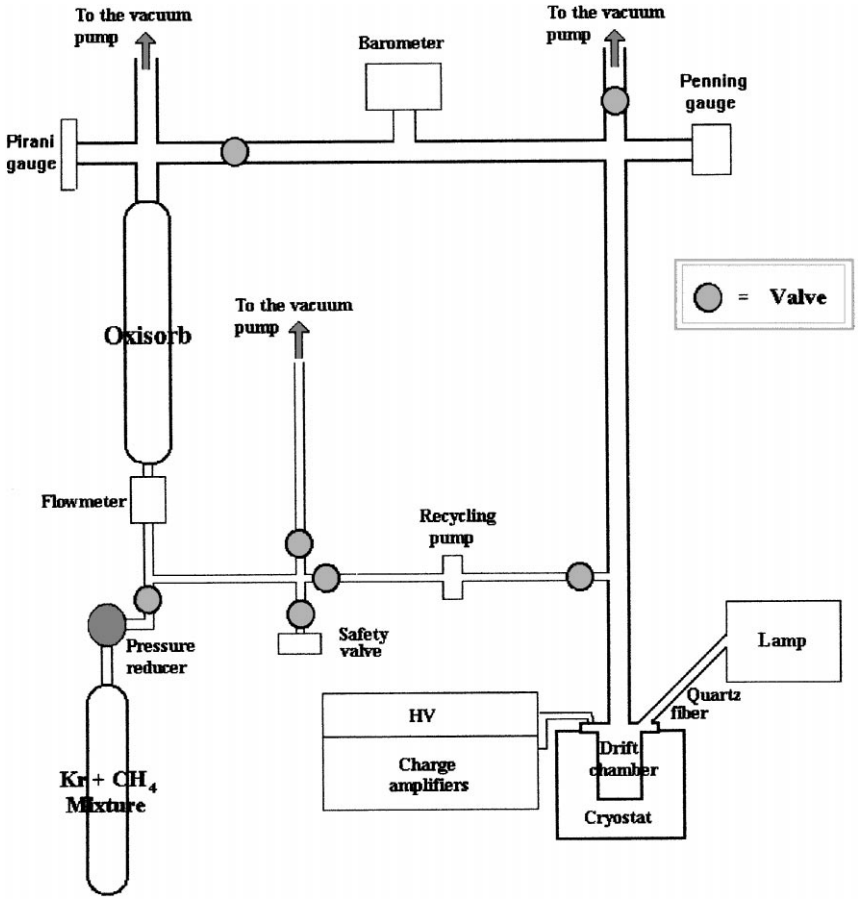

Fig. 3. Gas purification system and cryogenics.

The fact that we did not need any overpressure ensures that the methane present in the gaseous mixture liquefies together with the krypton.

2.3. Electronics and acquisition system

We collect, process and record signals from the cathode, the anode and from both grids. These signals, after AC coupling, are integrated by charge-sensitive amplifiers designed for liquid krypton calorimetry [13]. A calibration circuit, integrated in the amplifiers, provides the correspondence between pulse height and collected charge, essential for the measurement of lifetime. The decay time constant of the amplifier has been set at 300 μs, its maximum possible value, to allow a correct measurement of the longest (some tens of μs) drift times.

The choice of charge-sensitive amplifiers is made necessary by the amount of charge we are able to extract from the cathode by photoelectric effect: due to the UV lamp limited power and long pulse width , the average emitted electron current is not suitable for current-sensitive amplifiers.

Amplifier pulses were digitized at a frequency of 100 MHz (one measurement every 10 ns) by a digital oscilloscope and then sent to a PC, on which the analysis is performed. A schematic drawing of the acquisition system is shown in Fig. 4.

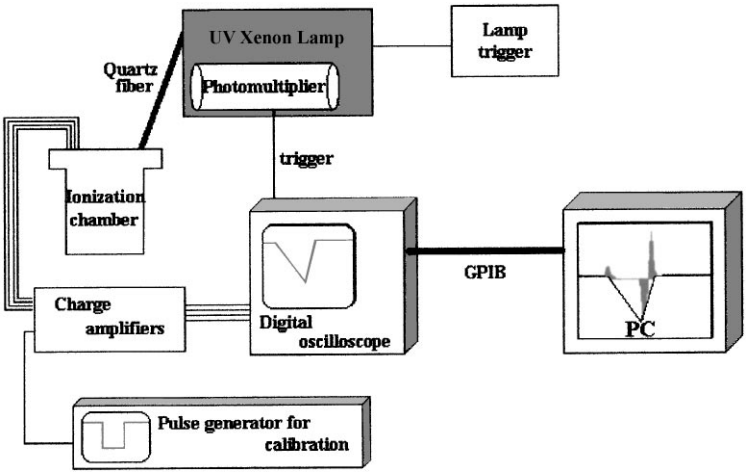

Fig. 4. Acquisition system.

3. Data taking

Data have been taken for pure krypton and for krypton with 1%, 2%, 3%, 5% and 10% methane. Typical pressures range from 3 to 5 atm (absolute). No dependence of velocity from pressure has been found. Pressure matters however, since the higher the pressure the wider the temperature range over which the krypton is liquid (it is about 22°C at 3 atm, and 30°C at 5 atm).

A significant dependence of velocity from temperature is observed in pure krypton, as formerly noted by other authors [14,15]. Our data confirm the measurements of Kalinin et al. [15]. No such a dependence is, in first approximation, observed in LKr–methane mixtures, but further investigations are in progress.

A typical measurement takes about 5 h, over which the temperatures and the pressure are recorded. Data have been taken with two different HV distributions:

- In the first set of data positive HV was applied to the anode and negative to the cathode, both up to 6 kV, and the drift time was measured over the 27 mm gap between the two grids, for fields up to 2000 V/cm.
- In the second set-up the negative HV was still applied to the cathode, while the positive HV was applied to the grid (GK) facing the cathode, so that in the 13 mm gap between cathode and its grid a much larger field (up to 9000 V/cm) was obtained.

The fields in the various regions have been computed taking into account the values of the resistors immersed in the liquid krypton at their appropriate temperatures. An error of 1% for data taken with the first set-up, 3% for data taken with second set-up, has been assigned to the values of the field: the main contributions are errors in measurement of these resistors and of the exact positions of the two grids.

In first HV set-up, for each value of electric field, four pulses are collected, one from each electrode; typical collected pulses are shown in Fig. 5. In the second HV set-up only pulses from cathode and GK have been collected. For reduction of electronic noise in data, each measured waveform is actually an average of typically 3000 individual signals.

4. Principle of measurement and analysis

4.1. Measuring drift velocity

A charge moving between two plane and parallel electrodes induces on them a current

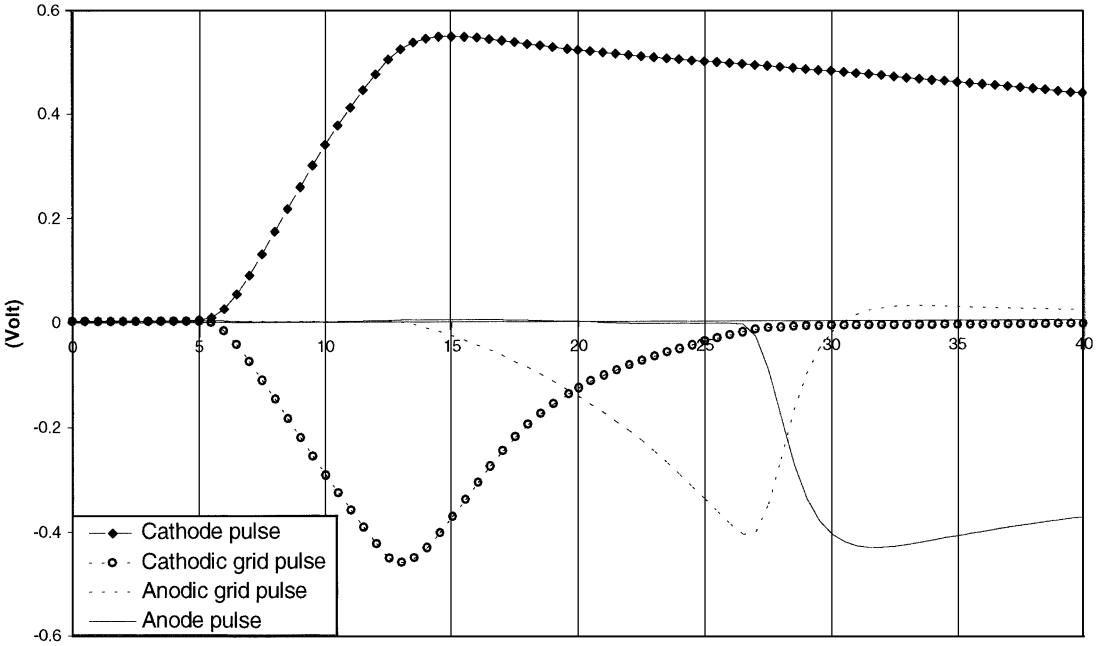

Fig. 5. Collected pulses in first HV setup.

given by [16]

$$i(t) = \frac{q(t)*v}{d} = \frac{q(t)}{t_d} \tag{1}$$

where $q(t)$ is the charge present at time t between the two electrodes, v is the charge drift velocity, d the distance between electrodes, and t_d the drift time.

Our drift time measurements are complicated by the fact that the light pulse is wide. Let $q(u)$ be the time distribution of the charge in the ionization chamber (which we assume to be the distribution of the light measured by the photomultiplier): the current $i(t)$ induced on the grid facing the cathode (GK) during data acquisition with the second HV set-up is then

$$i(t) = \begin{cases} \frac{v}{d}\int_0^t q(u)\,\mathrm{d}u & \text{if } t < t_d \\ \frac{v}{d}\left[\int_0^t q(u)\,\mathrm{d}u - \int_{t_d}^t q(u)\,\mathrm{d}u\right] & \text{if } t > t_d \end{cases} \tag{2}$$

where $t = 0$ corresponds to the departure of the first electron from the cathode, and t_d is drift time between cathode and GK. If the charge bunch has a time width smaller than the drift time the previous formula can be approximated by

$$i(t) = \begin{cases} \frac{v}{d}\int_0^t q(u)\,\mathrm{d}u & \text{if } t < t_d \\ \frac{v}{d}\left[Q_{tot} - \int_{t_d}^t q(u)\,\mathrm{d}u\right] & \text{if } t > t_d \end{cases} \tag{3}$$

where Q_{tot} is the total charge extracted from the cathode. These currents are then integrated by the charge amplifiers. Similar formulas hold for the other three signals.

Therefore, by deriving twice the amplifier signals we obtain the charge bunch shape as it is collected by an electrode or as it is passing through a grid; and we are able to identify the instant in which the maximum of the charge bunch arrives on each electrode (see Fig. 6).

A double derivation, however, increases enormously the effect of electronic noise. In order to reduce it, two different analysis algorithms have been used:

- "moving average" on 25 points corresponding to 250 ns (applicable on long drift times, i.e. drift

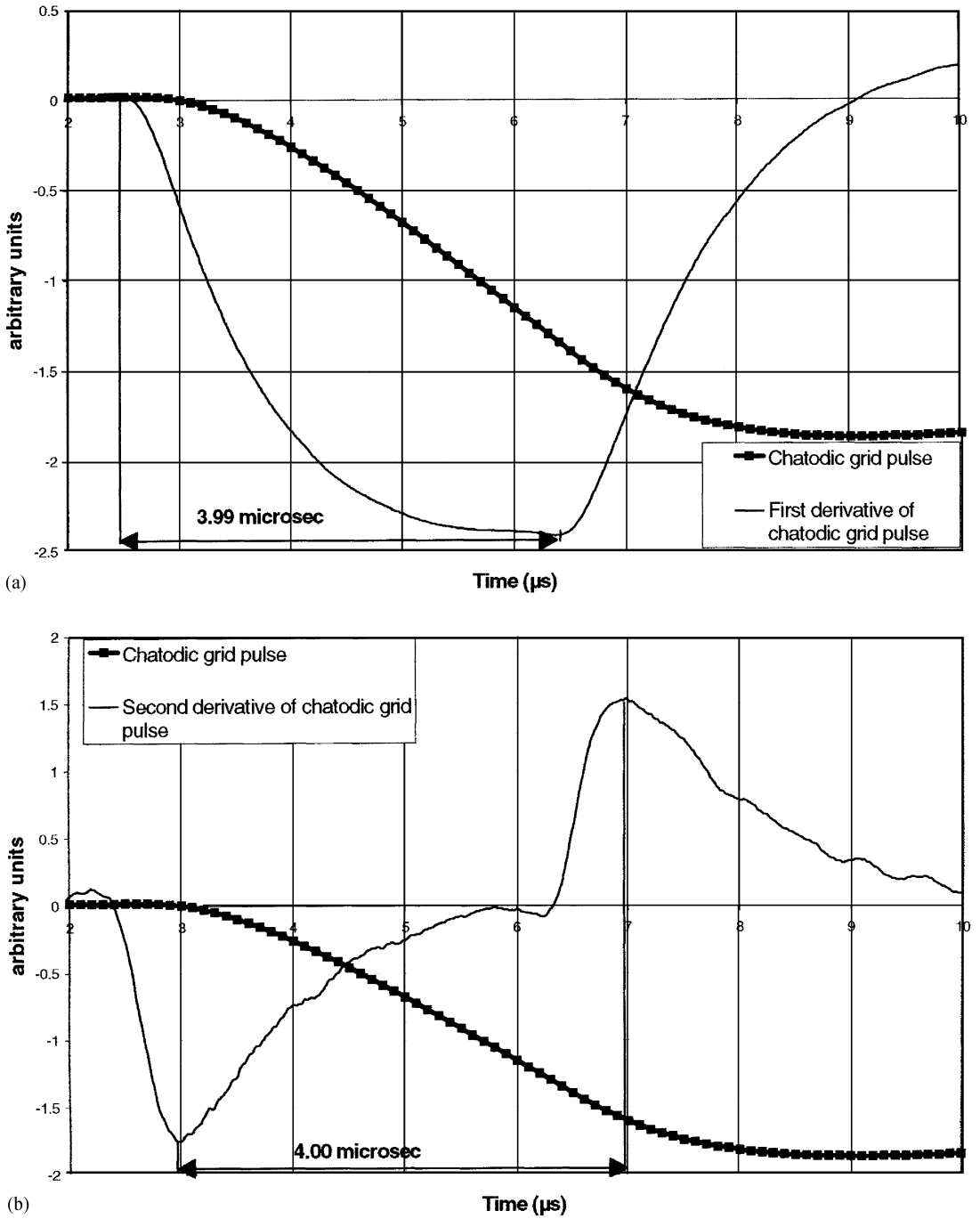

Fig. 6. Comparison between the two different ways of measuring drift time: (a) using edges of first derivative; (b) using minima/maxima of second derivative computed using moving average algorithm: the minimum of the second derivative corresponds to the maximum of the charge bunch leaving the cathode, the maximum to its arrival on GK.

time measurements in the first HV set-up): each data point is replaced the average of the 25 points around it;
- Fourier transform with damping of higher frequencies (applicable to short drift times, i.e. data from the second HV set-up).

The first algorithm consists in applying the moving average on the signal, then deriving a first time, moving average on the derivative, deriving a second time and applying the moving average again. Such an algorithm is applicable only on signals with long drift times (order of some μs). Only in such case the signals are not deformed by the moving average. To check this fact we have simulated signals from the ionization chamber by integrating Eq. (2) for various values of the drift time t_d. Fig. 7 shows the effect of the application of this algorithm on an anodic grid pulse.

The second algorithm consists in computing the Fourier transform of the signal with the FFT algorithm, applying an exponential suppression of the frequencies greater than a cut-off frequency, and transforming back the frequency spectrum into a signal, which is then much cleaner and can be derived twice. The threshold frequency is typically 1.5 MHz. In this case too simulation confirms that the algorithm does not affect the correct measurement of drift times.

The measurements of the times of emission from cathode, collection on anode or traversal of the grids done so far are taken on the passage of the *maximum* of the charge bunch and are therefore affected by a rather large error. We have assigned to the times measured in this way an error typically of $\pm$ 30 ns or, in same cases, where the noise was large, up to 50 ns.

However, in order to check the procedure we have also, for a few pulses, measured the times by detecting the instant of the beginning of emission (traversal, collection) of charge. We have used for this the first derivatives of the signals, which are proportional to the detected currents, and have measured the sudden change in slope of such pulses (Fig. 6a). As shown by Fig. 6 the measured times are practically the same as those from the first algorithm. We have also verified that the finite time response of the amplifiers does not affect the measurement of drift time – in both algorithms.

The uncertainty on measured drift-time varies from $\pm$ 42 to $\pm$ 70 ns, corresponding to an error on velocity varying from 1% to 3% for measurements with first HV set-up, from 2% to 10% for measurements with the second HV set-up.

For drift times of the same order of the width of the electron bunch we have corrected the data for the fact that while the second electrode is collecting the first arriving electrons, new ones are emerging from the first electrode. This causes a deformation on the second derivative of the signals which would give a measured drift time longer than the real one. We have simulated the effect and obtained the correction to apply to data, which is never larger than 4%.

4.2. Measuring electron lifetime

By measuring the ratio between charge collected by the anode Q_A and charge emitted by cathode Q_C, we can estimate the electron lifetime τ in liquid krypton–methane mixtures:

$$\frac{Q_A}{Q_C} = e^{t_d/\tau}. \quad (4)$$

In practice the lifetime has been estimated using the first HV set-up, at an electric field between grids of 150 V/cm. At this value of the field we have a quite good charge collecting efficiency and a long drift time.

5. Results

In Figs. 8 and 9 we present measured drift velocities versus electric field in three different field ranges: low fields (10–500 V/cm), medium fields (10–2000 V/cm), high fields (100–9000 V/cm). The first two data sets are taken using the first HV set-up, while high fields results are obtained with the second HV set-up. The three sets match in the region of common electric fields as shown in Fig. 10. For comparison the NA48 data [2] in pure LKr are also shown.

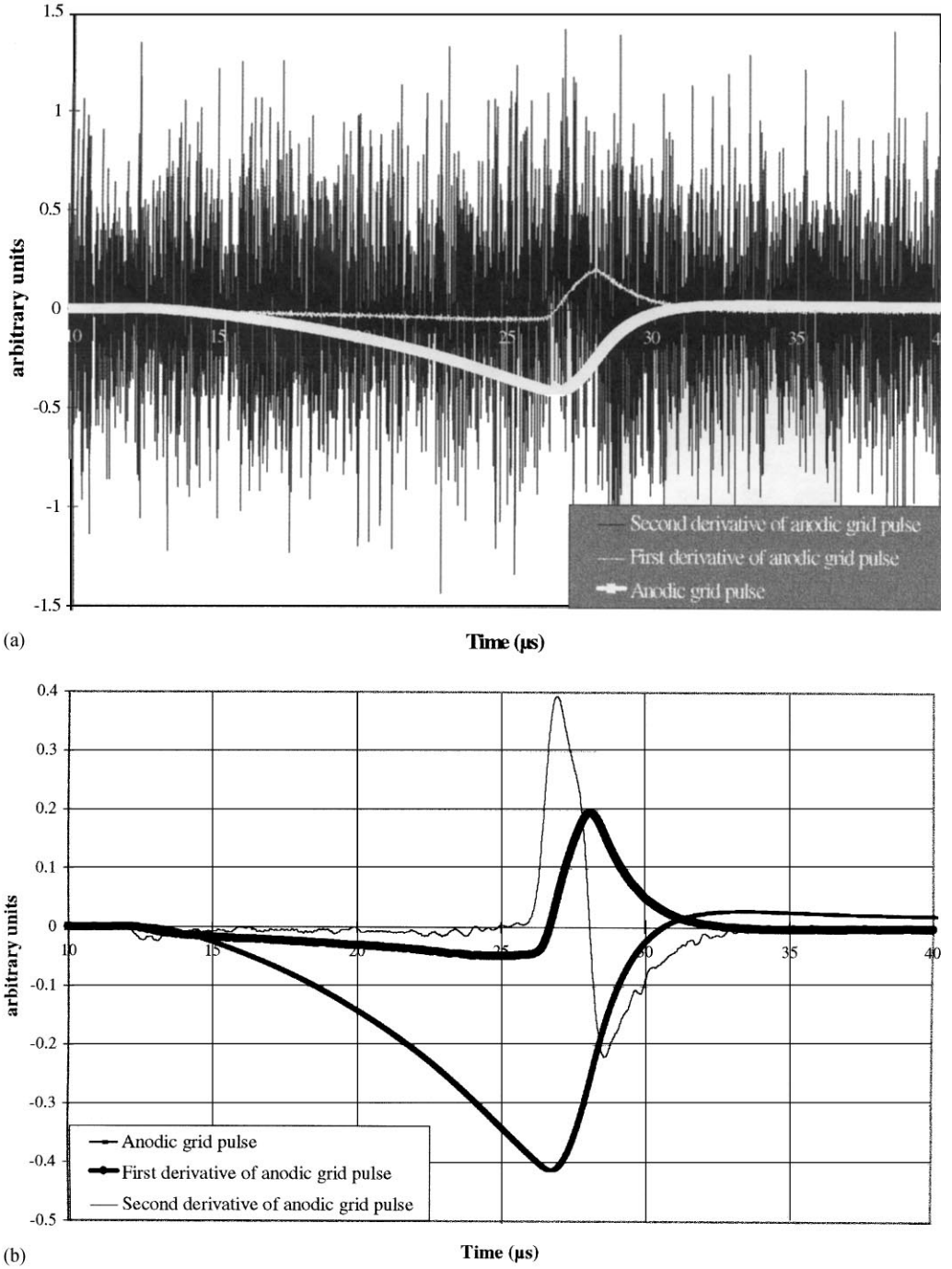

Fig. 7. (a) Effects of electronic noise on second derivative of an anodic grid pulse, (b) the noise is removed by the "moving average" algorithm.

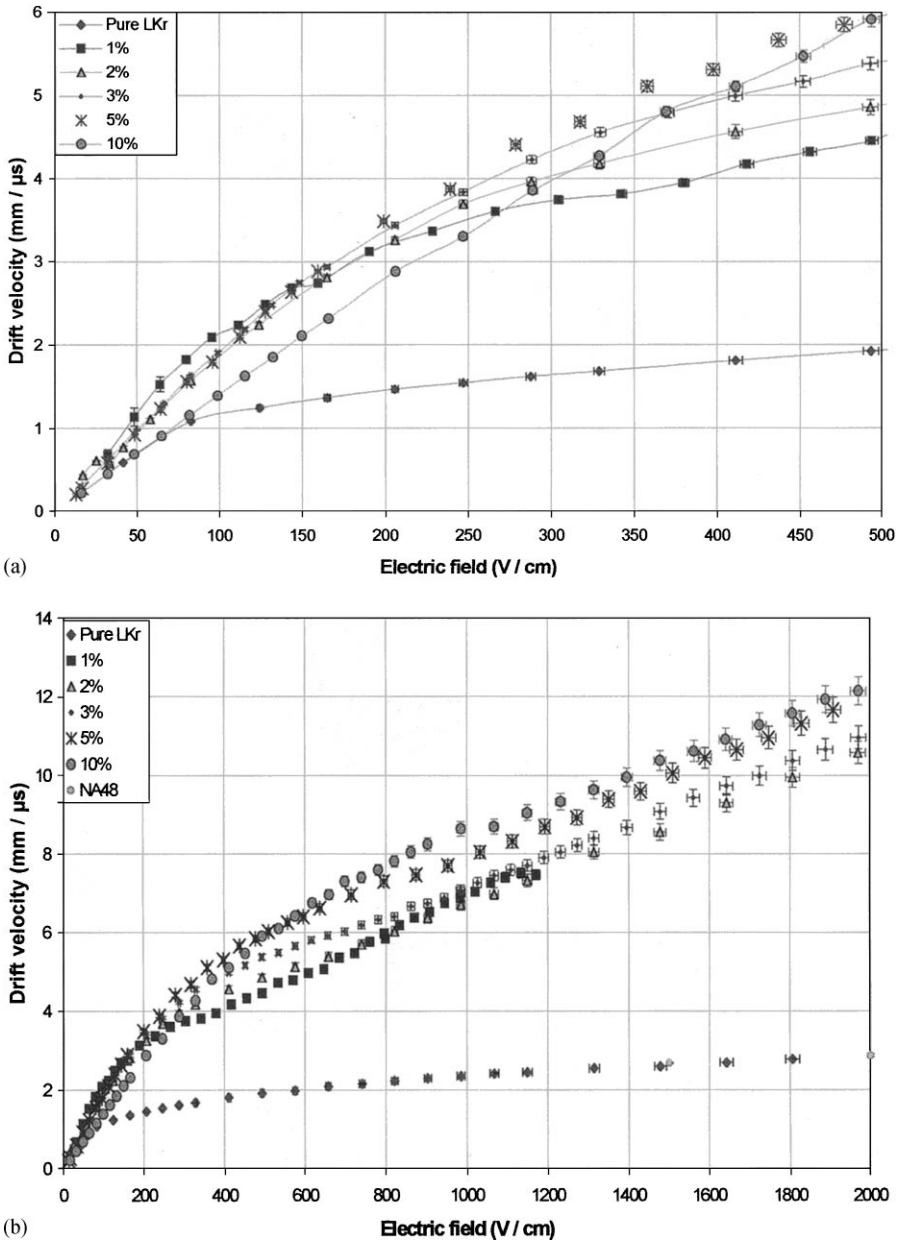

Fig. 8. Electron drift velocity in LKr–methane mixtures versus electric field. Data from the first HV setup at: (a) low electric fields (10–500 V/cm) and (b) medium electric fields (10–2000 V/cm). Lines are reported only as eye-guide. Error bars are indicated wherever they are larger than the symbols.

In Fig. 11 we plot the electron mobilities computed from our data versus electric field, and in Fig. 12 the dependence of electron drift velocity from both electric field and methane percentage. Finally in Fig. 13 the effect of methane addition to LKr can be seen from a direct comparison of anode pulses collected with and without methane.

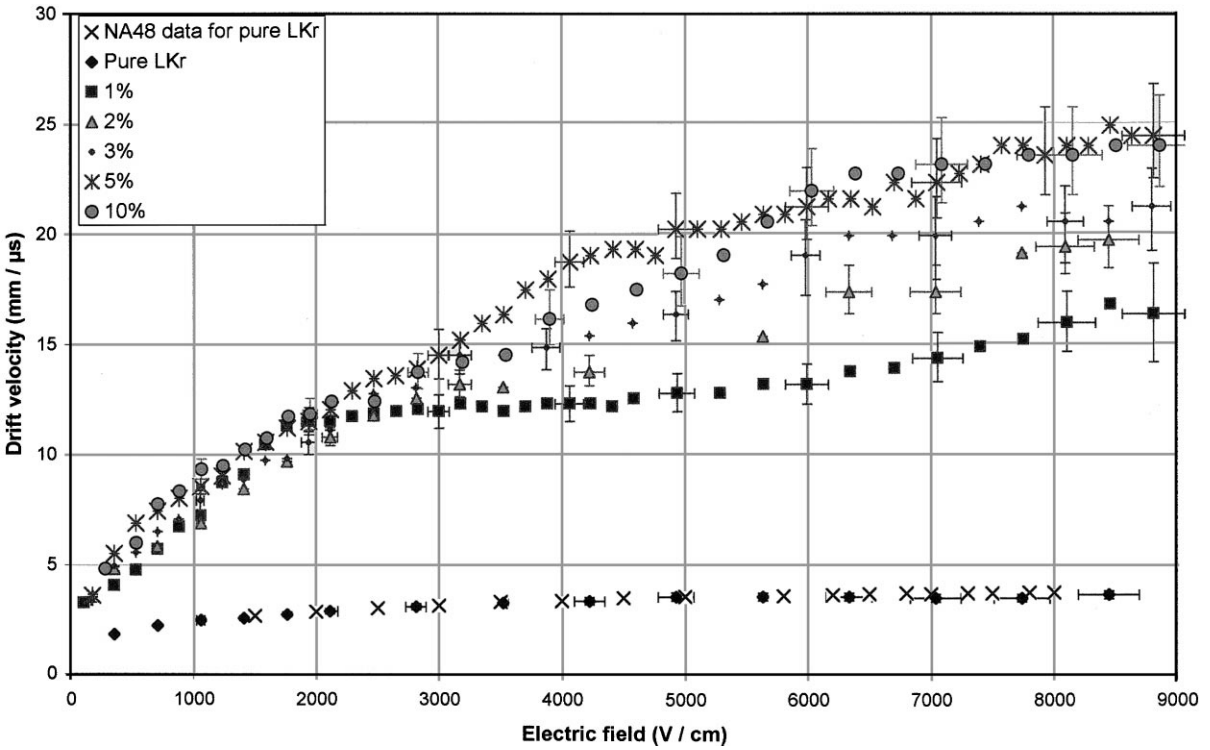

Fig. 9. Electron drift velocity in LKr–methane mixtures versus electric field. Data from the second HV setup at high electric fields (100–9000 V/cm). Error bars are indicated only on some points to avoid confusing the figure.

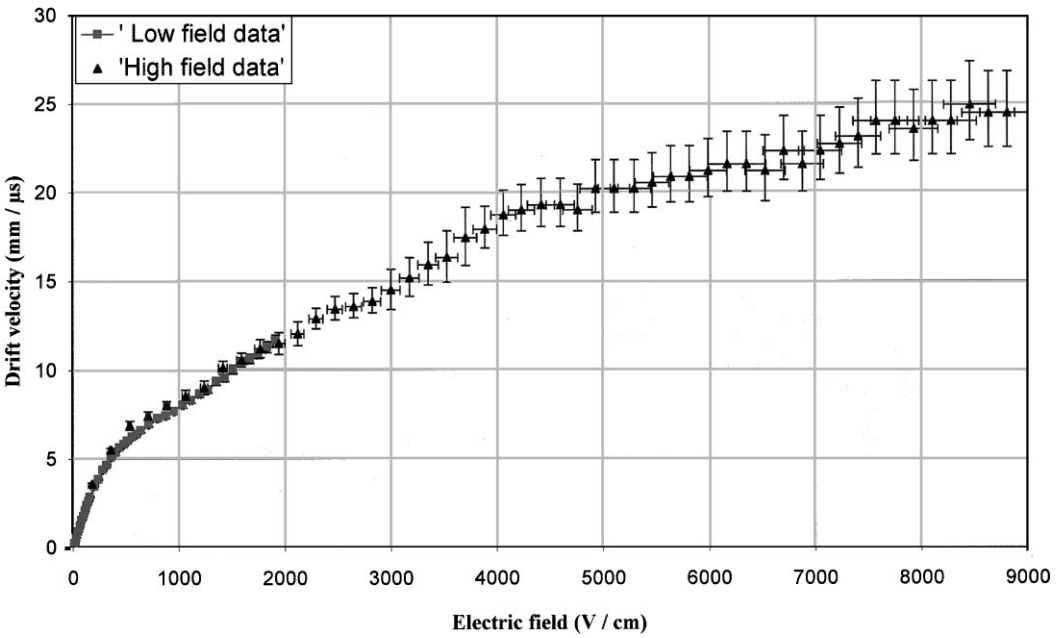

Fig. 10. Electron drift velocities in a mixture of LKr and methane at 5%. Matching of the data series acquired with the two different HV setup.

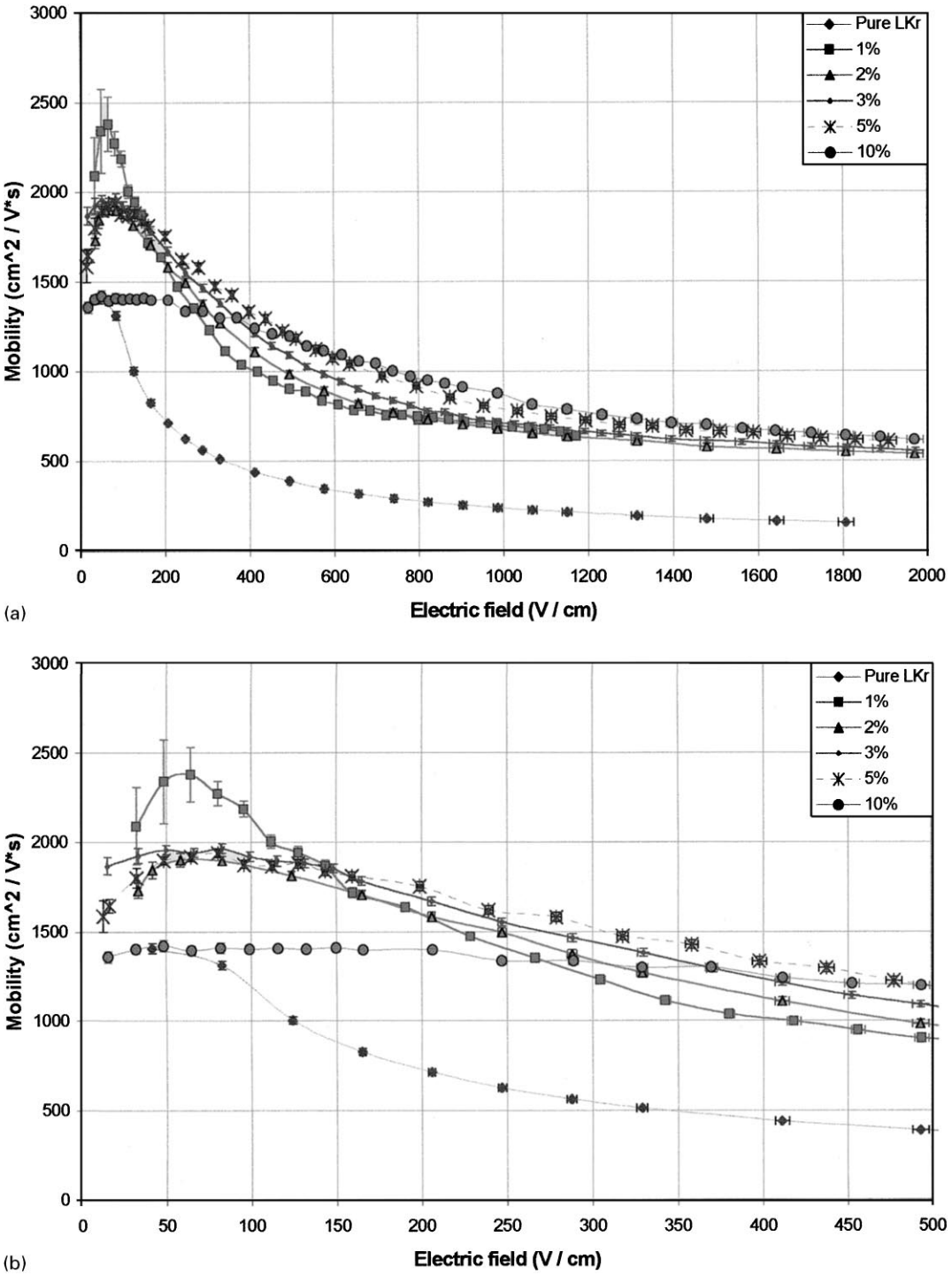

Fig. 11. Electron mobility in LKr–methane mixtures versus electric field at: (a) medium electric fields (10–2000 V/cm) and (b) low electric fields (10–500 V/cm). Lines are reported only as eye-guide.

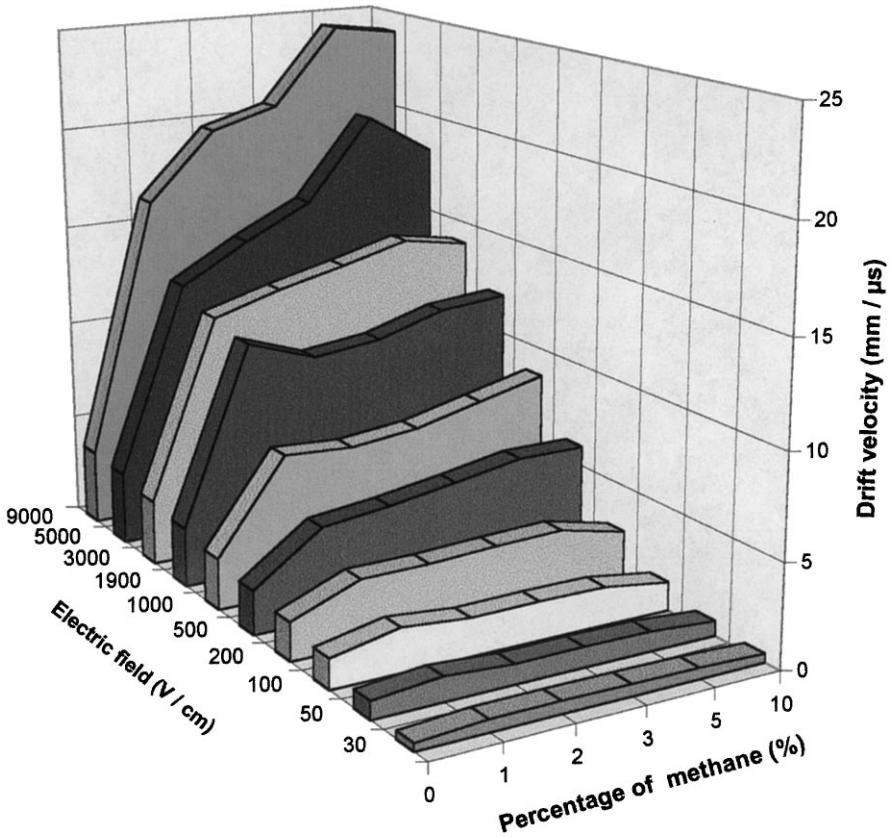

Fig. 12. Electon drift velocity as a function of electric field and methane fraction.

The dependence of the electron drift velocity on electric field and methane concentration can be roughly described in the following way:

Methane has different effects on the drift velocity, depending on the regime of the electron drift motion and hence on the value of the electric field:

- in the low electric field region, where the mobility is constant, the higher the dopant concentration the lower the electron mobility (Fig. 11);
- the larger the methane percentage the wider the electric field region in which mobility is constant (this effect is especially evident for the 10% methane data, see Fig. 11);
- at high field the higher the methane concentration the higher the electron drift velocity: at 9 kV/cm we observe an increase up to a factor 6 in drift velocity from pure liquid krypton to 5% or 10% LKr–methane mixtures

This behaviour can be qualitatively explained if we recall the models of electron transport phenomena in liquids:

- According to Itoh et al. [17] at low electric fields (virtually at null field) liquefied noble gases as Ar, Kr and Xe can be described using the band theory developed by solid state physicists. In this picture electron scattering is produced by local fluctuation of the energy V_0 of the bottom of the conduction band, due to local fluctuations of numerical density and solute concentration. In our case by increasing methane concentration we increase concentration fluctuations and therefore scattering of electrons, reduce their mean free path and eventually their mobility.

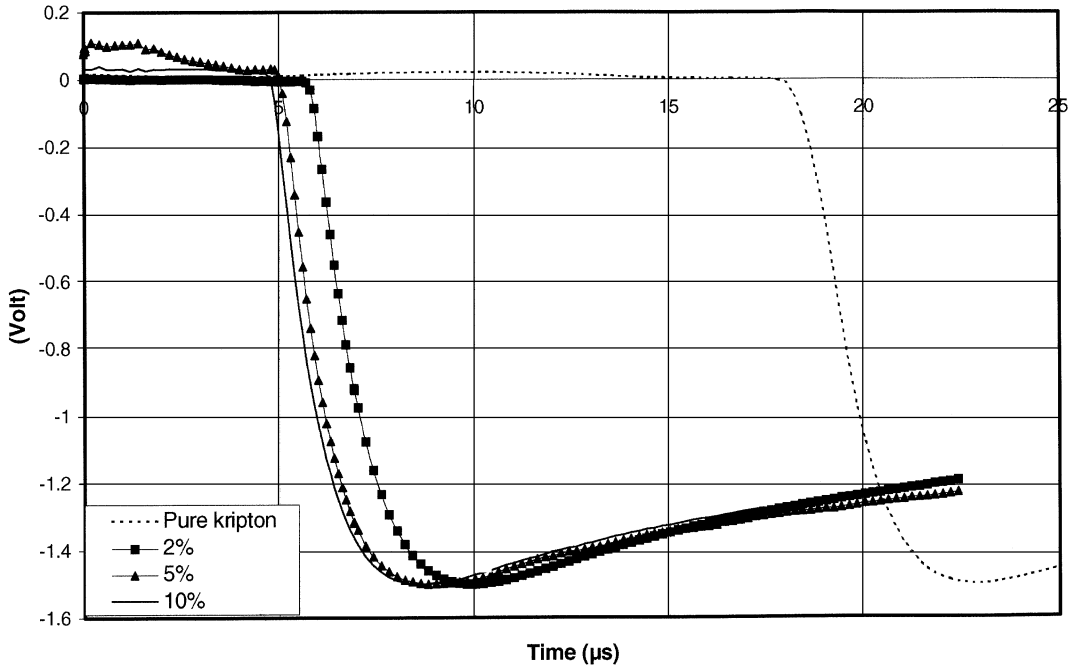

Fig. 13. Anode pulses collected with the same electric field configuration at different concentrations of methane in the gaseous mixture. The electric field between grids is 1.3 kV/cm.

- At high field, according to the gas kinetic theory approach to transport phenomena in liquids [18], the drift velocity is, in first approximation, given by

$$v_{\mathrm{d}} = \frac{1}{2} a \tau_e = \frac{1}{2} \frac{eE\tau_e}{m} = \frac{1}{2} \frac{eE}{m} \left\langle \frac{l_e}{v_{\mathrm{T}}} \right\rangle \tag{5}$$

where a is the acceleration due to the electric field, τ_e the mean free time between two successive scatterings, e is the electron charge, E the electric field, m the electron mass, l_e the mean free path, and v_{T} the electron thermal velocity. Methane is an organic compound, whose molecules have vibrational and rotational degrees of freedom. When an electron scatters on such molecules it transfers in average a significant part of its energy, ending with a lower thermal velocity and consequently with a larger drift velocity. What happens is, in fact, that the electric field region in which electrons are "thermal", that is the electric field range in which the mobility is constant, becomes significantly wider.

Finally, in a mixture of LKr and methane at 5%, we have measured an electron lifetime larger than 210 μs. We are able to give only a lower limit because our apparatus is insensitive to larger values of electrons lifetime.

6. Conclusions

We have studied the effect of the addition of a complex molecule – methane – on the electron drift velocity in liquid krypton over a large range of electric fields. We confirm what has already been seen with other combinations of noble liquids and hydrocarbons, an increase of the drift velocity at high fields. Such increase can be very large: we observe up to a factor 6 with high methane concentrations and large fields. At lower fields, in the regime of constant mobility, we observe smaller mobilities and a wider region of constant mobility. Finally, we do not observe any appreciable reduction of electron lifetime in the liquid due to methane introduction.

Acknowledgements

The authors express their thanks to Dr. Gianni Carugno who helped them with many discussions in the initial stage of the project, and to Prof. A. F. Borghesani for theoretical discussions.

References

[1] T. Doke, Nucl. Instr. and Meth. A 337 (1993) 113.
[2] G D. Barr et al., Nucl. Instr. and Meth. A 370 (1996) 413.
[3] V.M. Aulchenko et al., Nucl. Instr. and Meth. A 316 (1992) 8.
[4] The Atlas Collaboration, Nucl. Instr. and Meth. A 384 (1996) 230.
[5] P. Benetti et al., Nucl. Instr. and Meth. A 327 (1993) 173.
[6] D.C. Rahm, Nucl. Instr. and Meth. A 316 (1992) 67.
[7] V. Vuillemin et al., Nucl. Instr. and Meth. A 316 (1992) 71.
[8] J. Séguinot et al., Nucl. Instr. and Meth. A 323 (1992) 583.
[9] K. Yoshino et al., Phys. Rev. A 14 (1976) 438.
[10] R. Holroyd, W. Schmidt, Ann. Rev. Phys. Chem. 40 (1989) 439.
[11] O. Bunemann et al., Canad. J. Res. 27 A (6) (1949) 191
[12] M. Griesheim, Industrial Gas Division, Dusseldof, Germany.
[13] V.M. Aulchenko et al., Nucl. Instr. and Meth. A 327 (1993) 193.
[14] P.K. Lebedev, S.V. Muraviev, Fifth International Conference on Instrumentation for Colliding Beam Physics, INP Novosibirsk, 1993, p. 371.
[15] A.M. Kalinin et al., CERN NA-48 note 96/8.
[16] E. Gatti et al., Nucl. Instr. and Meth. 193 (1982) 651.
[17] K. Itoh, M. Nishikawa, R. Holroyd, Phys. Rev. B 44 (1991) 12680.
[18] K. Kaneko, Y. Usami, K. Kitahara, J. Chem. Phys. 89 (1988) 6420.